In Vitro and In Vivo Comparison of Two Suprachoroidal Shunts

Julius T. Oatts,[1] Ze Zhang,[1] Harry Tseng,[2] M. Bruce Shields,[1] John H. Sinard,[3,4] and Nils A. Loewen[5]

[1]Yale University School of Medicine, New Haven, Connecticut
[2]Albany Medical College, Albany, New York
[3]Department of Ophthalmology and Visual Sciences, Yale University School of Medicine, New Haven, Connecticut
[4]Department of Pathology, Yale University School of Medicine, New Haven, Connecticut
[5]Department of Ophthalmology, University of Pittsburgh Medical Center, Pittsburgh, Pennsylvania

Correspondence: Julius T. Oatts, Department of Ophthalmology and Visual Sciences, Yale University School of Medicine, 300 George Street Suite 8100, New Haven, CT 06511; julius.oatts@yale.edu.

Submitted: February 11, 2013
Accepted: July 2, 2013

Citation: Oatts JT, Zhang Z, Tseng H, Shields MB, Sinard JH, Loewen NA. In vitro and in vivo comparison of two suprachoroidal shunts. *Invest Ophthalmol Vis Sci*. 2013;54:5416–5423. DOI:10.1167/iovs.13-11853

Purpose. To compare fibrosis, aqueous humor dynamics, and intraocular pressure (IOP) of two suprachoroidal shunts as part of a new class of glaucoma drainage devices.

Methods. Following proliferation analysis in vitro, 20 rabbits were implanted with either a gold shunt (GS, GMSplus+, SOLX) or a polypropylene shunt (PS, Aquashunt, OPKO). Ten eyes received mitomycin C (MMC) and triamcinolone. Peak and trough IOP were monitored with a pneumatonometer and tono-pen for 15 weeks. Aqueous humor dynamics were evaluated fluorophotometrically and tonographically. Fibrosis was quantified.

Results. In vitro proliferation was similar. In vivo, both shunts were devoid of foreign body reaction but exhibited fibrosis, and GS showed vascularization. There was no significant difference in aqueous or uveoscleral flow. Preoperative morning IOP was 23.7 ± 2 mm Hg, and evening IOP was 26.5 ± 2 mm Hg ($P = 0.000$). Morning IOP was decreased through 15 weeks and evening IOP through 8 weeks in all groups. The morning IOP decrease was most profound at 15 weeks in PS (41%) compared to GS (18%). Antifibrotics initially enhanced but eventually diminished shunt performance. At 15 weeks, thickness of scleral fibrosis was greater in GS (246 ± 47 μm) and PS (188 ± 47 μm, $P = 0.285$) compared with GS+MMC (109 ± 26 μm, $P = 0.023$ to GS) and PS+MMC (48 ± 30 μm, $P = 0.028$ to PS).

Conclusions. In a rabbit model, suprachoroidal polypropylene and gold shunts allow access to a new drainage pathway with different IOP profiles that can be modified with antifibrotics.

Keywords: suprachoroidal shunt, glaucoma drainage device, rabbit

The increasing burden of glaucoma,[1] which is a direct result of a longer life expectancy,[2] and the considerable risks of standard trabeculectomy and tube shunts[3] has led to a search for new surgeries for moderate and advanced disease stages. Because classical surgeries shunt aqueous humor to a subconjunctival or sub-Tenon pocket, fibrosis and infection remain a lifelong threat.[3] Suprachoroidal shunts have been developed in an attempt to avoid these problems by draining aqueous humor into a potential space on the inside of the eye, the suprachoroidal space, taking advantage of the hydrostatic pressure gradient between the anterior chamber and suprachoroidal space.[4]

In this study, we compared two suprachoroidal shunts, a gold shunt (GS; GMSplus+; SOLX Ltd., Waltham, MA) and a polypropylene shunt (PS; Aquashunt; OPKO Health, Miami, FL), examining in vitro and in vivo growth patterns of the cell types that come into direct contact with these devices. Using rabbits as a species that has very little natural uveoscleral outflow, we hypothesized that we could create a fibrosis-prone animal model to readily display differences in shunt function and the impact of antifibrotics on outflow. Because suprachoroidal shunts increase flow into the anatomic compartment that is primarily responsible for pressure-independent, uveoscleral outflow, we further hypothesized that suprachoroidal shunts would reduce IOP the most at a time of the day when this outflow contributes the least.

Methods

In Vitro Proliferation Studies

In vitro biocompatibility of suprachoroidal shunts was evaluated using cell lines of corneal endothelial, trabecular meshwork, and fibroblast origin that were transduced with feline immunodeficiency viral (FIV) vectors to stably express enhanced green fluorescent protein (eGFP) as described previously.[5,6] Briefly, feline kidney fibroblast (CrFK) (American Type Culture Collection, Manassas, VA), trabecular meshwork (NTM5) (gift from Alcon Laboratories, Fort Worth, TX), and bovine corneal endothelial (BCE) (American Type Culture Collection) cells were transduced with a multiplicity of infection (MOI) of 30 to achieve high and even expression levels followed by expansion.[5]

eGFP-expressing CrFK, BCE, and NTM5 cells were seeded onto GS and PS inside six-well plates at 75 cells/mm^2. Growth rate on these materials was compared to that in control wells by eGFP-optimized fluorescent image capture (Eclipse TE300; Nikon, Melville, NY).

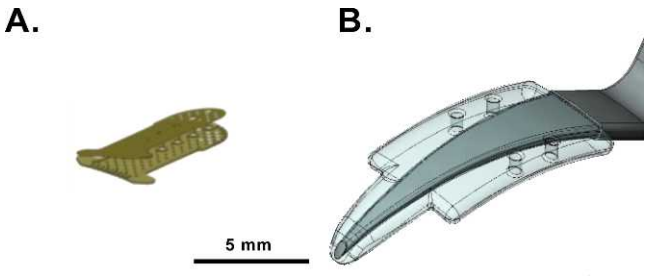

FIGURE 1. Suprachoroidal shunts in comparison: (**A**) gold shunt (GS); (**B**) polypropylene shunt (PS) on device inserter.

Study Design

Right eyes of 20 rabbits were implanted with GS or PS (Fig. 1) to have an 89% chance of detecting IOP differences of 3 ± 2 mm Hg or 93% for 5 ± 2 mm Hg (nonpaired *t*-test, alpha error 5%). GS was the most recent-generation device (GMSplus+; SOLX Ltd.) with an external size of $3.2 \times 5.2 \times 0.05$ mm^3, while PS (Aquashunt; OPKO Health) had an external size of $4 \times 10 \times 0.75$ mm^3. Half of each group ($n = 5$) received intraoperative, subconjunctival mitomycin C (MMC, 0.2 mg; Gemini Bio-Products, West Sacramento, CA) and intracyclodialysis cleft triamcinolone acetate (TAC, Triesence; Alcon Laboratories) to maximize antifibrotic and anti-inflammatory action. IOP was measured with both a pneumatonometer and tono-pen preoperatively and weekly postoperatively at peak and trough times for 15 weeks. Pneumatonometry and fluorophotometry were used to measure aqueous humor turnover and calculate outflow facility and uveoscleral flow. Fibrosis was analyzed and quantified using histology and morphometry at 15 weeks postoperatively.

Animals

Shunts were implanted in 6- to 7-week-old New Zealand white rabbits (Harlan, Indianapolis, IN) that were acclimatized for 1 week to a 12-hour light–dark cycle, with lights on at 7 AM at a room temperature of 20 ± 4°C, and housed in separate cages with food and water available ad libitum. All practices complied with the ARVO Statement for the Use of Animals in Ophthalmic and Vision Research and were approved by the Yale University Institutional Animal Care and Use Committee.

Suprachoroidal Shunt Implantation

Animals were anesthetized with intramuscular ketamine (35 mg/kg; McKesson, San Francisco, CA) and xylazine (5 mg/kg; Lloyd, Inc., Shenandoah, IA). The surgical eye was cleaned with ophthalmic beta-iodine (Betadine 5%; Alcon Laboratories) and draped sterilely, and a lid speculum was inserted. When macroscopic, microscopic, and functional data in pilot animals confirmed that a clear corneal insertion technique from within the anterior chamber was less traumatic and more reproducible than the transscleral approach used in humans, 20 animals were implanted using this new approach. A shelved, peripheral clear corneal incision was fashioned according to shunt size. The anterior chamber at the incision site was filled by 30% with viscoelastic (Ocucoat; Bausch & Lomb, Clearwater, FL) before the tip of the cannula was turned toward the iris root and used to gently create a cyclodialysis, injecting viscoelastic to safely expand this space. Shunts were delivered to the anterior chamber via the included inserter and then carefully retracted into the cyclodialysis cleft using a cystotome. The incision was closed with a 10–0 nylon suture. Half of each group of animals received 50 μL TAC in the suprachoroidal space. This transscleral injection was aimed at the midsection of the shunt using a 27-gauge needle in posterior, bevel-down position and applied after watertight closure when the eye was pressurized. These animals also received a subconjunctival injection of MMC. Postoperatively, all animals received moxifloxacin (Vigamox 0.5%; Alcon Laboratories) and prednisolone acetate 1% (Falcon Pharmaceuticals, Fort Worth, TX) every 12 hours for 7 days. Immediately postoperatively, a slit-lamp exam was performed to assess for ocular inflammation (cells or flare), corneal edema, or hyphema. This exam was also repeated at 1 week.

Structural Assessment

Device placement was confirmed by ultrasound biomicroscopy (UBM; UBM Plus; Accutome, Malvern, PA). Following anesthesia, a 20-mm eye cup was inserted between the eyelids and filled with saline solution. With a 48-MHz transducer, scanning was performed under standardized room lighting conditions. Cross-sectional and transverse images were obtained detailing the device in relation to the suprachoroidal space as well as other anatomical landmarks including cornea, iris, ciliary body, anterior chamber angle, and peripheral sclera. Central corneal thickness (CCT) was measured by ultrasound pachymetry (Pachmate; DGH Technology, Exton, PA) in triplicate in the morning and evening, corresponding with peak and trough IOP measurements.[7]

Functional Assessment

IOP measurements were performed in conscious rabbits gently restrained by hand. Rabbits received one drop of topical anesthesia with proparacaine 0.5% (Akorn, Inc., Lake Forest, IL). All pressures were obtained using both pneumatonometry (model 30 pneumatonometer; Reichert Technologies, Depew, NY) and tono-pen applanation (Tono-Pen Avia; Reichert Technologies) during the same measurement session.

Animals were acclimated to IOP measurements daily for 1 week before preoperative diurnal pressures were recorded. IOP was measured every 3 hours from 0800 (8 AM) until 2300 (11 PM) for 48 hours to establish preoperative diurnal patterns. IOP was then measured weekly at peak and trough pressure through 15 weeks postoperatively. Because IOP measured with the pneumatonometer was considerably higher throughout the day and more sensitively displayed circadian IOP fluctuation than measurements with the tono-pen (Supplementary Fig. S1), statistical analysis was carried out with pneumatonometric data.

Anterior segment fluorescence was measured in triplicate with a scanning ocular fluorophotometer (Fluorotron Master; OcuMetrics, Mountain View, CA). Measurements were taken between 1000 (10 AM) and 1800 (6 PM) and repeated at 1-hour intervals for four sets of scans to determine aqueous flow (F_a).[7] Following the fourth measurement, animals received intramuscular acetazolamide (16 mg/kg; X-Gen Pharmaceuticals, Big Flats, NY) to calculate fluorophotometric outflow facility (C_{fl}) using two more scans 2 hours later and 1 hour apart.[7]

Tonographic outflow facility (C_{ton}) was evaluated by 2-minute constant-pressure tonography and calculated as the ratio of the change in aqueous volume to the change in IOP during the 2-minute measurement.[8] Uveoscleral outflow (F_u) was calculated using the modified Goldmann equation and an episcleral venous pressure of 12 mm Hg.[9] When C_{fl} was used, IOP was measured prior to acetazolamide administration; when C_{ton} was used, IOP was the pneumatonometric IOP before the start of tonography.

Investigative Ophthalmology & Visual Science

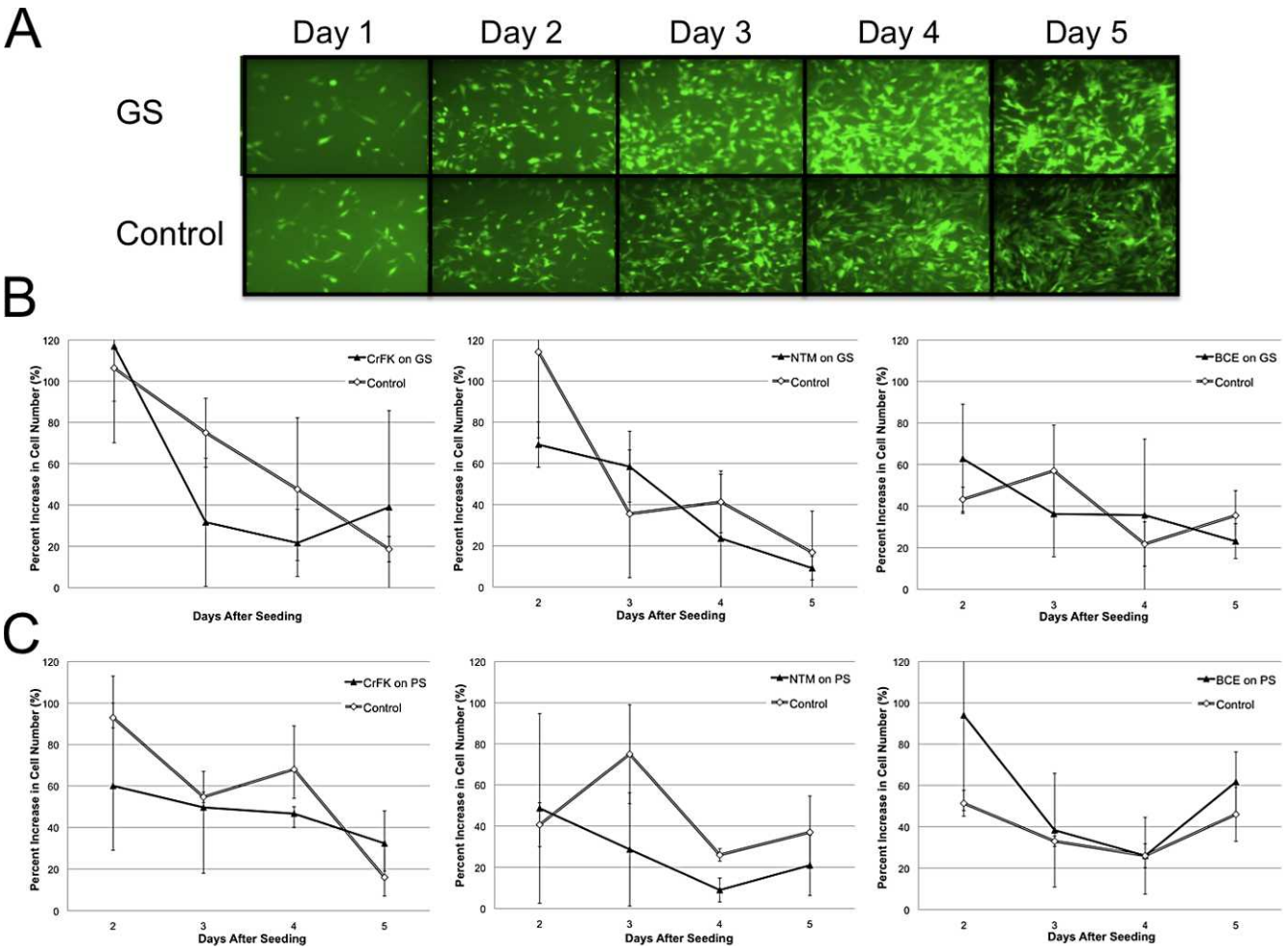

FIGURE 2. In vitro biocompatibility test using newly generated, stably eGFP-expressing cell lines (CrFK, fibroblasts; NTM, trabecular meshwork cells; BCE, endothelial cells; $N = 3$). Because shunts are not translucent, a reflection-based fluorescence assay had to be developed. (**A**) Example of transduced CrFK cells on GS. Graphic representations of cell growth rates on days 2 through 5 after seeding on GS (**B**) and PS (**C**).

Histology

At the study endpoint of 15 weeks, eyes of euthanized animals (120 mg/kg phenobarbital via ear vein, Euthasol; Virbac, Fort Worth, TX) were enucleated and fixed in 10% formalin for 2 to 3 days. After fixation, the eyes were hemisected and stereomicroscopy was performed. The device and surrounding tissue were excised as a block, processed, and paraffin embedded. Sequential 5-μm sections were cut and stained with hematoxylin and eosin (H&E). Thirty minutes prior to euthanization, two or three anesthetized rabbits in each group received a 0.2-mL intracameral cationic ferritin tracer (10 mg/mL, pH 5.8; Sigma-Aldrich, St. Louis, MO) to assess outflow function by histology.[10] In addition to standard H&E staining, these slides were also stained with Prussian blue to highlight ferritin deposition.

Fibrosis was measured on both scleral and choroidal sides of the shunt using ImageJ 1.46 (National Institutes of Health, Bethesda, MD) on digital photomicrographs. Due to the difference in cellular architecture, fibrotic tissue developing following insertion of the device was easily differentiated from normal sclera and choroid. All measurements were taken in the middle of the device, and reported values were obtained as the average of fibrosis thickness across three sections from each specimen.

Statistics

IOP, outflow facility, and uveoscleral flow were analyzed with repeated-measures analysis of variance (ANOVA). Student's paired *t*-tests were used to compare diurnal IOP, aqueous flow, outflow facility (both fluorophotometric and tonographic), uveoscleral flow, and CCT intraindividually. Student's unpaired *t*-tests were used to compare these parameters and fibrosis between groups. All data are presented as the mean ± standard deviation (SD) and were considered statistically significant at $P < 0.05$.

RESULTS

In cell culture, fibroblasts, trabecular meshwork, and corneal endothelial cells reached full confluence within 5 days of seeding without signs of cytotoxicity or restricted growth compared to controls. Image analysis showed that there were no significant differences in growth rates between cells seeded on gold, polypropylene, or control tissue culture plates (Fig. 2).

Following acclimatization, rabbits displayed a preoperative diurnal IOP variation, with pressure highest in the evening and lowest in the morning (Fig. 3). Average morning IOP was 23.7 ± 2 mm Hg at 0800 (8 AM), and evening IOP was 26.5 ± 2 mm Hg at 2000 (10 PM) ($P = 0.000$).

Investigative Ophthalmology & Visual Science

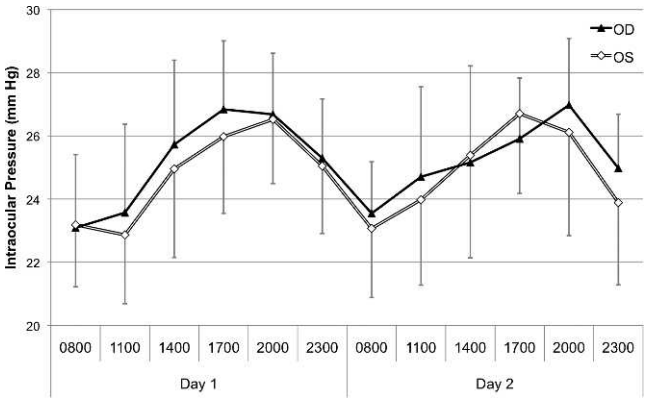

Figure 3. Preoperative diurnal pneumatonometric IOP by time of day.

Two pilot animals served to develop an ab interno, intracameral, suprachoroidal shunt implantation technique for the rabbit when transscleral insertion was found to be traumatic and highly variable in this species. Implantation took approximately 20 minutes in each of the 20 subsequent animals. A limited intraoperative hyphema was observed in 5 animals, 4 of which had eyes implanted with PS. One animal experienced a retinal detachment secondary to PS implantation. Of 10 PS implanted, 2 progressively migrated toward the anterior chamber. Of the 10 animals treated with adjuvant MMC and TAC, 3 implanted with GS had shallow, diffuse blebs during the early postoperative period, 2 of which resolved within 2 weeks postoperatively. In the third GS animal, the bleb persisted until postoperative week 6, at which point the IOP increased. One PS animal without MMC and TAC also had a postoperative bleb.

Compared with preoperative IOP, morning IOP was decreased through 15 weeks and evening IOP through 8 weeks in all groups ($P < 0.05$). The morning IOP decrease was most profound at 15 weeks in PS (41%) compared to GS (18%). In the intereye comparison, all groups showed a consistent decrease in both morning and evening IOP through postoperative week 4 ($P < 0.05$), except at 1 week in the GS group (Fig. 4). Evening IOP showed a more gradual return to baseline pressure through postoperative 15 weeks as compared to morning IOP (Fig. 4). Compared to values in control eyes, morning IOP was reduced in PS through 15 weeks, in PS+MMC through 7 weeks, and in GS+MMC through 3 weeks ($P < 0.05$). The decrease in evening IOP remained significant through 4 weeks in both MMC groups, through 15 weeks in PS, and nonsignificant in the GS group.

There was no difference in aqueous flow (F_a) between groups preoperatively, with an average of 3.3 ± 0.7 μL/min. Compared to the control eyes, F_a was not different in shunt eyes at any time point. Average preoperative tonographic outflow facility (C_t) was 0.31 ± 0.09 μL/min/mm Hg. The only

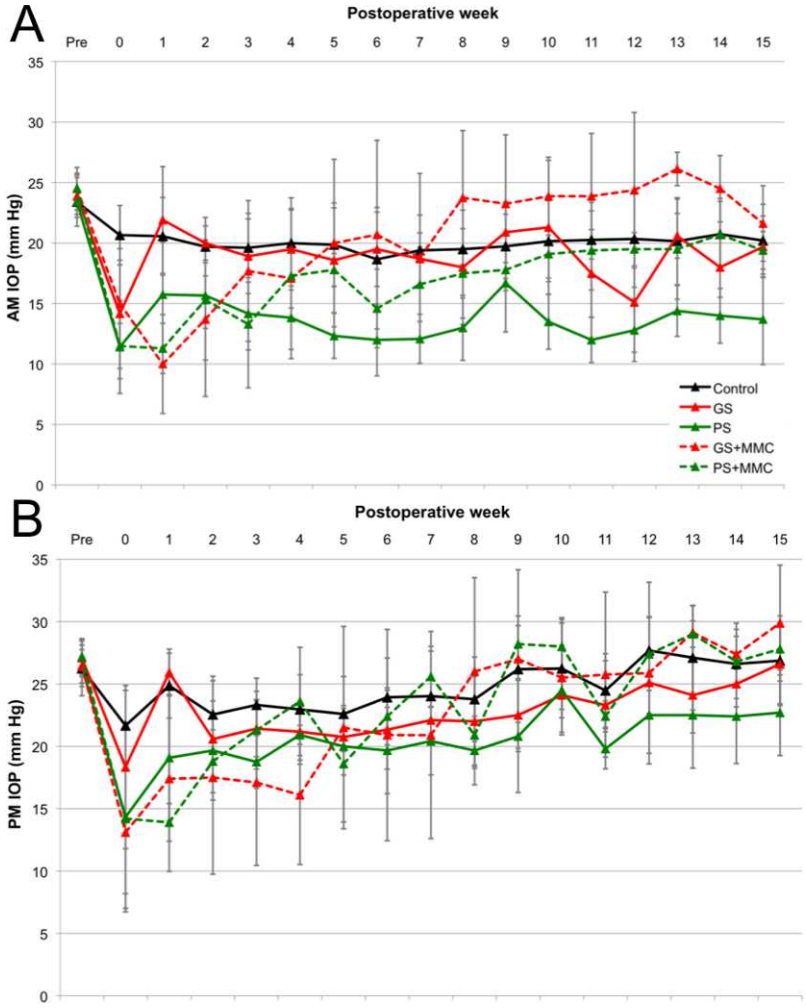

Figure 4. Intraocular pressure (IOP) through week 15 in the morning (**A**) and evening (**B**).

Investigative Ophthalmology & Visual Science

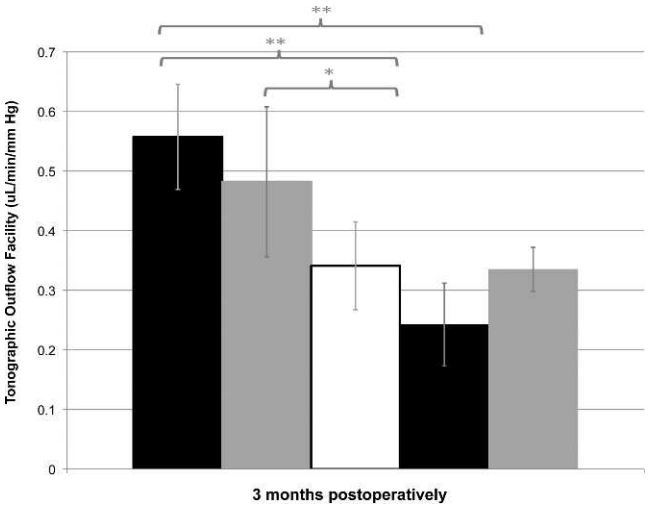

FIGURE 5. Tonographic outflow facility (C_t) in all groups at 3 months postoperatively. $^*P < 0.05$, $^{**}P < 0.01$.

significant difference was found at 3 months, when both groups receiving antimetabolites exhibited greater C_t than control groups (control, 0.34 ± 0.16 μL/min/mm Hg; GS+MMC, 0.56 ± 0.13 μL/min/mm Hg, $P = 0.007$; PS+MMC, 0.48 ± 0.14 μL/min/mm Hg, $P = 0.049$) (Fig. 5).

Average preoperative tonographic uveoscleral flow (F_{ut}) was 2.02 ± 1.30 μL/min. At 3 months postoperatively, GS+MMC and PS+MMC exhibited a small but significant decline compared to GS and PS.

Interventions changed both the average preoperative fluorophotometric outflow facility (C_f) of 0.18 ± 0.5 μL/min/mm Hg and fluorophotometric uveoscleral flow (F_{uf}) of 1.35 ± 5.71 μL/min over a wide range that was not statistically significant.

No adverse effects on corneal endothelial function as measured by CCT was observed. Rabbits exhibited a diurnal variation in CCT, with preoperative morning CCT of 362 ± 15 μm and evening CCT of 333 ± 12 μm. In all groups, physiologic diurnal differences, with CCT larger in the morning than in the evening, were maintained through 3 months postoperatively. Device implantation had no effect on corneal thickness through 3 months. Compared to that in control eyes, CCT in implanted eyes was not significantly different at 1 month (GS, $P = 0.307$; PS, $P = 0.918$) or 3 months (GS, $P = 0.772$; PS = 0.663). Similarly, evening CCT was not significantly different at 1 month (GS, $P = 0.341$; PS, $P = 0.982$) or 3 months (GS, $P = 0.165$; PS = 0.462). UBM visualization of suprachoroidal lakes (not shown) and stereomicroscopic examination of dissected eyes confirmed proper device implantation in all animals (Fig. 6).

Vascularization could be occasionally observed at the tail of both shunt types (Figs. 6D, 6E), while a suprachoroidal drainage pocket was observed extending from the tail of the GS (Fig. 6C). There were extensive anterior synechiae at the GS implantation site of the eye that experienced an IOP elevation following bleb disappearance at week 6 and corresponding buphthalmic changes.

Histologically, all GS and PS were in the suprachoroidal space and devoid of foreign body reaction. All specimens exhibited fibrosis that was thicker on the scleral side than on the choroidal side of the device. Fibrosis was more dense at the tail of the device and was less compact but thicker toward the head. GS eyes showed histiocytic inflammation, which was not found in GS eyes that received MMC or in any PS eyes.

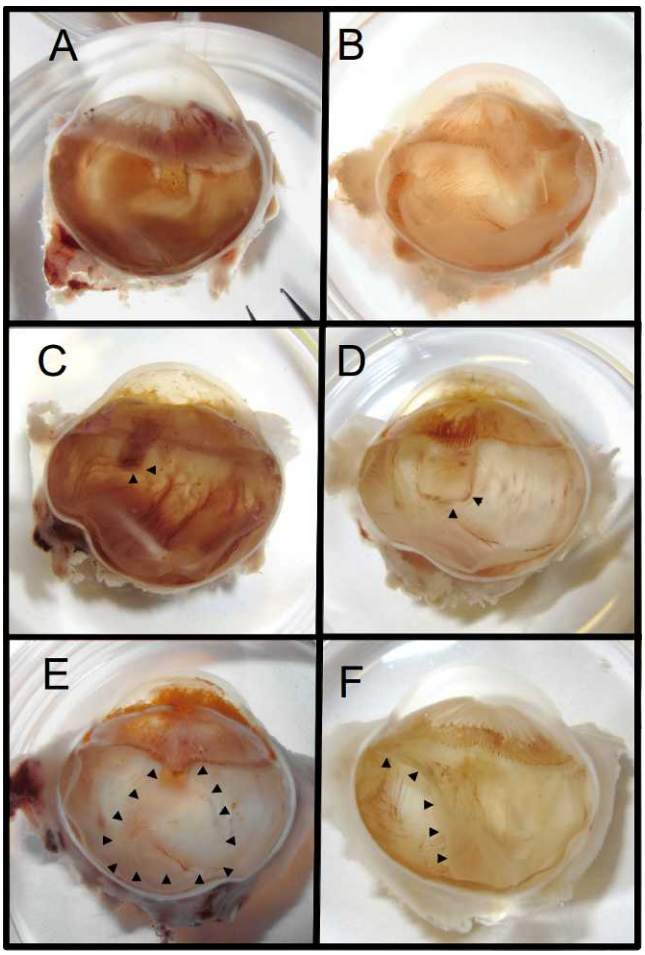

FIGURE 6. Stereomicroscopic images showing shunts in hemisected eyes. Representative presentation of GS (**A**) and PS (**B**). GS (**C**) and PS (**D**) with vascularization engulfing tail (*arrowheads*). GS with suprachoroidal drainage pocket (**E**, *arrowheads*) and retinal detachment in eye implanted with PS (**F**, *arrowheads*).

In GS, regardless of the addition of antimetabolites, fibrovascular tissue had grown into the pores of the shunt and was present within the lumen (Fig. 6). At 15 weeks postoperatively, fibrosis on the scleral side of the shunt was greater in GS (246 ± 47 μm) and PS (188 ± 47 μm, $P = 0.285$) compared to GS+MMC (109 ± 26 μm, $P = 0.023$ to GS) and PS+MMC (48 ± 30 μm, $P = 0.028$ to PS) (Fig. 7).

At 15 weeks, fibrosis on the choroidal side of the shunt was less in all groups (range 17–22 μm) without a difference between groups ($P > 0.05$). Ferritin outflow tracer was seen surrounding both PS and GS in the suprachoroidal space, including at the tail end of devices, despite fibrovascular tissue in the lumen (Fig. 8B). GS specimens showed relatively large, thin-walled vascular structures within the device (Fig. 8, inset).

DISCUSSION

Fibrosis and foreign body reaction in the suprachoroidal space have not been formally examined, though the development of novel drainage devices depends on them. This study systematically compared two different suprachoroidal shunt designs and materials both in vitro and in vivo. The original idea of lowering IOP with a cyclodialysis cleft was complicated by unpredictable closure,[11] and cleft maintainers introduced to prevent this were not tolerated well.[12] Advances in material

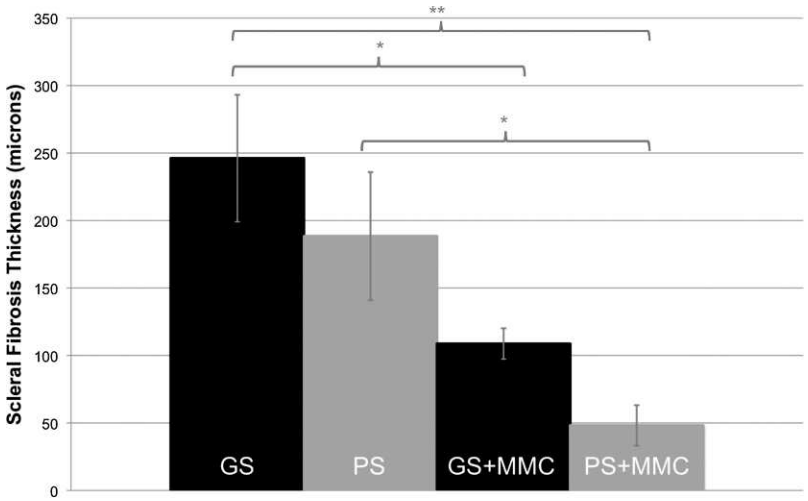

Figure 7. Graph showing the thickness of scleral fibrosis in all groups 15 weeks postoperatively. Mean ± SEM. $^{*}P < 0.05$, $^{**}P < 0.01$.

sciences and microengineering can now achieve reduced bioreactivity and size. In order to display differences in biocompatibility and shunt function more readily, we chose the rabbit. In this species, wound healing and fibrosis occur rapidly, causing glaucoma surgeries such as trabeculectomies to fail within several days.[13] Rabbits have only limited uveoscleral outflow,[14] potentially making enhancement of this route even more apparent. We assessed in vitro growth patterns of cell types that make contact with suprachoroidal shunts to assess material properties before in vivo studies. Because neither shunt was sufficiently translucent, we developed a reflection-based fluorescent assay with FIV-mediated[5,15] stably eGFP-expressing cell lines of fibroblast, trabecular meshwork, and endothelial origin enabling cell counts and direct observation of growth patterns.

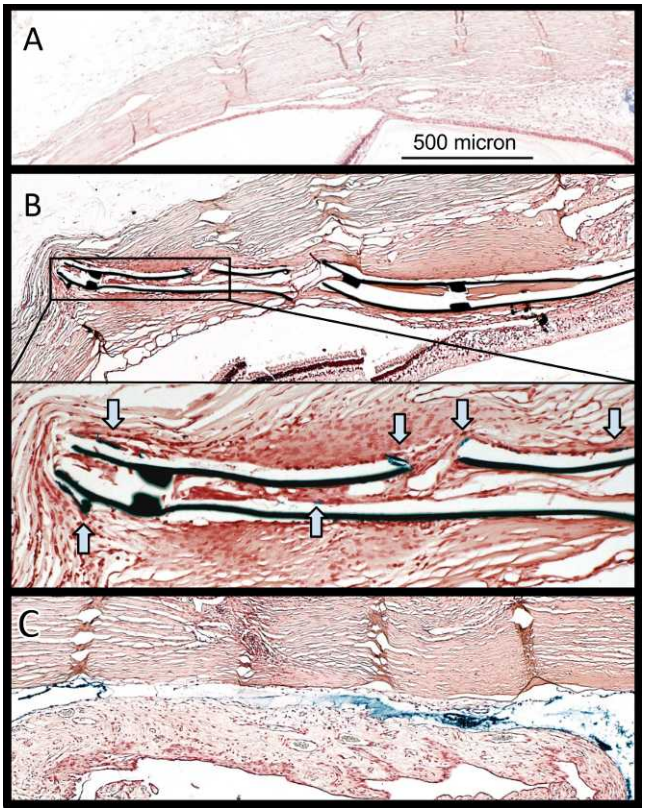

Figure 8. Histology of implantation site. Light microscope images showing Prussian blue–stained slides. (**A**) Control eye. (**B**) GS-implanted eye shows blue tracer along the implant despite vessels in shunt lumen (inset, magnified view; *blue arrows*, tracer). Thin-walled, large vascular structures may resemble lymphatic vessels more than blood vessels. (**C**) PS surrounded by prominent fibrosis. The polypropylene dissolved in processing, while the space remains outlined by tracer.

As a chemically nonreactive precious metal that can be manufactured so as to be devoid of nanostructures that encourage cell migration and differentiation,[16–19] gold had been postulated to have ideal features for a suprachoroidal shunt but required the use of pure elemental gold to eliminate traces of toxic copper.[20] The resulting low hardness[21] necessitated a photolithographic etching technique to provide internal pillars to resist torque. In contrast, the polypropylene of the PS shunt is a thermoplastic polymer that can be melt processed by extrusion and is flexible and inexpensive, but has nanoscale grooves that may offer more points of adhesion compared to gold.[22] Despite these distinct differences, the cell growth patterns we observed were very similar.

Animals exhibited a known 24-hour IOP pattern,[23] validating our measurements. We found a considerable difference in the initial comparison of pneumatonometer and tono-pen in the rabbit, which may be the result of a CCT that is only approximately 60% of that in humans,[24] affecting both methods differently. The length of IOP reduction with both GS and PS was longer than the days to weeks that are achievable by trabeculectomy and other glaucoma surgeries in this species.[10,13,25] GS lowered IOP significantly primarily in the evening from postoperative weeks 6 through 11. In contrast, PS resulted in significantly lower IOP more often in the morning than in the evening. This might well be a result of the different means through which these devices gain access to outflow routes and how they contribute to IOP during different times of the day. Histology indicated that GS may have developed a different, more fibrovascular access to the pressure-independent uveoscleral outflow as compared to PS, which had more classical bleb wall features. IOP in PS compared to GS may be lower as a result of the different absorption area and be less affected by fibrosis, as pressure, filtration space, and transmural gradient are closely related.

Our attempt to extend and enhance device function with adjuvant MMC and TAC caused a notable IOP decrease only during the first 4 weeks in GS and the first 7 weeks in PS, but

Investigative Ophthalmology & Visual Science

IOP was less than in non-MMC animals thereafter. The results for MMC and TAC with conventional glaucoma drainage devices have been similarly sobering,[26] possibly because in addition to fibrosis seen in blebs following trabeculectomy, a foreign body reaction to the shunt could play a role.[27] Surprisingly, we did not observe a foreign body reaction, though other mechanisms could explain a worse long-term IOP in eyes receiving MMC and TAC: As seen on slit-lamp exam in one animal with a bleb, channels toward the subconjunctival space might have formed in the early postoperative period and prevented the establishment of proper suprachoroidal drainage. Increased tonographic outflow facility in these eyes is consistent with this hypothesis, indicating that aqueous humor was displaceable even in animals without a visible bleb, possibly through needle tracks in the presence of reduced wound healing. Increased IOP can then result when the bleb disappears. Additionally, TAC could have worsened trabecular outflow over time,[28] while MMC may have caused avascularity in the area applied,[29] reducing uveoscleral outflow.

The present standard for implantation of both the GS and PS in clinical trials in humans is transscleral insertion; but in the rabbit, such an ab externo approach is rather traumatic due to a thin, friable sclera with firmly adherent uvea. We developed an ab interno insertion technique with well-controlled viscohydraulic expansion of the suprachoroidal space and positioning of the shunt, allowing us to standardize insertion and achieve consistent results. CCT was unaffected by the shunt and maintained a normal diurnal cycle.[7] In attempting to determine the mechanism of IOP reduction by GS and PS, we found that these surgeries induced considerable perturbations in fluorophotometric outflow measurements with standard deviations that were too large to allow detection of statistical significance.

Consistent with the idea of reduced fibrosis in the suprachoroidal space, fibrosis on the choroidal side of these shunts measured only 20 μm, while that on the scleral side was 200 to 250 μm, similar to that seen in external drainage surgery.[30,31] This remarkable difference between the two sides may be a direct result of the types and numbers of cells that the shunt is in contact with: The internal sclera is the same fibroblast-rich structure that affects external drainage surgery, while the highly vascularized choroid is detached from the scleral bed and contains fewer fibroblasts. Similar to findings from our in vitro experiments, no significant differences were seen between GS and PS, although PS was 25% thinner on average; this could be a result of aqueous humor flow and pressure gradient,[32–34] as the surface area of the GS is 20 times smaller compared with PS. GS-implanted eyes displayed ingrowth of a mixed fibrovascular tissue, but this did not prevent tracer flow as far as the tail. The vascular profiles identified included some with histologic features of blood vessels (with narrow, normal endothelium and basement membrane, and red blood cells in the lumen) and others more consistent with lymphatic vessels (with thin endothelium, poorly developed basement membrane, and no red blood cells visible). These could represent new structures that provide access to uveoscleral drainage routes.

In summary, the suprachoroidal shunts studied here lowered IOP with different profiles and up to seven times longer than trabeculectomy in this species. Fibroblast, trabecular meshwork, and endothelial cell growth indicated similar in vitro biocompatibility. In vivo, fibrosis occurred more on the scleral than on the choroidal side of the shunt and was observed inside the lumen of the gold shunt as well. The larger polypropylene shunt lowered pressure more and longer than the gold shunt but had more severe complications, which were also more frequent. The use of mitomycin C and triamcinolone worsened IOP response. Tracer experiments demonstrated shunt function up to the experimental endpoint of 15 weeks. In the absence of a significant decrease in aqueous humor production or increased trabecular flow, the main mechanism of IOP lowering was likely an increase in uveoscleral outflow.

Acknowledgments

Disclosure: **J.T. Oatts**, None; **Z. Zhang**, None; **H. Tseng**, None; **M.B. Shields**, P; **J.H. Sinard**, None; **N.A. Loewen**, SOLX (F)

References

1. Congdon N, O'Colmain B, Klaver CC, et al. Causes and prevalence of visual impairment among adults in the United States. *Arch Ophthalmol*. 2004;122:477–485.
2. Oeppen J, Vaupel JW. Demography. Broken limits to life expectancy. *Science*. 2002;296:1029–1031.
3. Gedde SJ, Heuer DK, Parrish RK II. Review of results from the Tube Versus Trabeculectomy Study. *Curr Opin Ophthalmol*. 2010;21:123–128.
4. Emi K, Pederson JE, Toris CB. Hydrostatic pressure of the suprachoroidal space. *Invest Ophthalmol Vis Sci*. 1989;30:233–238.
5. Loewen N, Fautsch MP, Teo WL, Bahler CK, Johnson DH, Poeschla EM. Long-term, targeted genetic modification of the aqueous humor outflow tract coupled with noninvasive imaging of gene expression in vivo. *Invest Ophthalmol Vis Sci*. 2004;45:3091–3098.
6. Saenz DT, Barraza R, Loewen N, Teo W, Poeschla EM. Feline immunodeficiency virus-based lentiviral vectors. *Cold Spring Harb Protoc*. 2012;2012:71–76.
7. Zhao M, Hejkal JJ, Camras CB, Toris CB. Aqueous humor dynamics during the day and night in juvenile and adult rabbits. *Invest Ophthalmol Vis Sci*. 2010;51:3145–3151.
8. Langham ME, Edwards N. A new procedure for the measurement of the outflow facility in conscious rabbits. *Exp Eye Res*. 1987;45:665–672.
9. Zamora DO, Kiel JW. Topical proparacaine and episcleral venous pressure in the rabbit. *Invest Ophthalmol Vis Sci*. 2009;50:2949–2952.
10. Lei J, Sun N, Zhao X, Kang Q, Chen L, Fan X. Morphologic study of the drainage pathway using a tracer after a bypass filtering procedure in rabbit eyes. *Ophthalmic Surg Lasers Imaging*. 2011;42:254–262.
11. Fuchs E. Ablösung der Aderhaut nach Staaroperation. *Graefes Arch Clin Exp Ophthalmol*. 1900;51.
12. Gills JP, Paterson CA, Paterson ME. Mode of action of cyclodialysis implants in man. *Invest Ophthalmol*. 1967;6:141–144.
13. Seetner A, Morin JD. Healing of trabeculectomies in rabbits. *Can J Ophthalmol*. 1979;14:121–125.
14. Toris C. Chapter 7. Aqueous humor dynamics I: measurement methods and animal studies. *Curr Top Membr*. 2008;62:193–229.
15. Loewen N, Bahler C, Teo WL, et al. Preservation of aqueous outflow facility after second-generation FIV vector-mediated expression of marker genes in anterior segments of human eyes. *Invest Ophthalmol Vis Sci*. 2002;43:3686–3690.
16. Lee MR, Kwon KW, Jung H, et al. Direct differentiation of human embryonic stem cells into selective neurons on nanoscale ridge/groove pattern arrays. *Biomaterials*. 2010;31:4360–4366.
17. Xie C, Hu J, Ma H, et al. Three-dimensional growth of iPS cell-derived smooth muscle cells on nanofibrous scaffolds. *Biomaterials*. 2011;32:4369–4375.

Investigative Ophthalmology & Visual Science

18. Russell P, Gasiorowski JZ, Nealy PF, Murphy CJ. Response of human trabecular meshwork cells to topographic cues on the nanoscale level. *Invest Ophthalmol Vis Sci*. 2008;49:629–635.
19. Kim DH, Lipke EA, Kim P, et al. Nanoscale cues regulate the structure and function of macroscopic cardiac tissue constructs. *Proc Natl Acad Sci U S A*. 2010;107:565–570.
20. McGahan MC, Bito LZ, Myers BM. The pathophysiology of the ocular microenvironment. II. Copper-induced ocular inflammation and hypotony. *Exp Eye Res*. 1986;42:595–605.
21. Soratur S. *Essentials of Dental Materials*. New Delhi, India: Jaypee Brothers Medical Publishers; 2002:341.
22. Dasari A, Rohrmann J, Misra RDK. Micro- and nanoscale evaluation of scratch damage in poly(propylene)s. *Macromol Mater Eng*. 2002;287:889–903.
23. Bar-Ilan A. Diurnal and seasonal variations in intraocular pressure in the rabbit. *Exp Eye Res*. 1984;39:175–181.
24. Brandt JD, Gordon MO, Gao F, et al. Adjusting intraocular pressure for central corneal thickness does not improve prediction models for primary open-angle glaucoma. *Ophthalmology*. 2012;119:437–442.
25. DeCroos FC, Ahmad S, Kondo Y, et al. Expanded polytetrafluoroethylene membrane alters tissue response to implanted Ahmed glaucoma valve. *Curr Eye Res*. 2009;34:562–567.
26. Al-Mobarak F, Khan AO. Two-year survival of Ahmed valve implantation in the first 2 years of life with and without intraoperative mitomycin-C. *Ophthalmology*. 2009;116:1862–1865.
27. Maumenee AE. External filtering operations for glaucoma: the mechanism of function and failure. *Trans Am Ophthalmol Soc*. 1960;58:319–328.
28. Jones R, Rhee DJ. Corticosteroid-induced ocular hypertension and glaucoma: a brief review and update of the literature. *Curr Opin Ophthalmol*. 2006;17:163–167.
29. Hardten DR, Samuelson TW. Ocular toxicity of mitomycin-C. *Int Ophthalmol Clin*. 1999;39:79–90.
30. Prata JA, Minckler DS, Mermoud A, Baerveldt G. Effects of intraoperative mitomycin-C on the function of Baerveldt glaucoma drainage implants in rabbits. *J Glaucoma*. 1996;5:29–38.
31. Takeuchi K, Nakazawa M, Yamazaki H, et al. Solid hyaluronic acid film and the prevention of postoperative fibrous scar formation in experimental animal eyes. *Arch Ophthalmol*. 2009;127:460–464.
32. Georgoulas S, Dahlmann-Noor A, Brocchini S, Khaw PT. Modulation of wound healing during and after glaucoma surgery. *Prog Brain Res*. 2008;173:237–254.
33. Loeffler KU, Jay JL. Tissue response to aqueous drainage in a functioning Molteno implant. *Br J Ophthalmol*. 1988;72:29–35.
34. Radius RL, Herschler J, Claflin A, Fiorentino G. Aqueous humor changes after experimental filtering surgery. *Am J Ophthalmol*. 1980;89:250–254.

Investigative Ophthalmology & Visual Science